eISSN 1303-1775 • pISSN 1303-1783

Neuroanatomy (2006) 5: 12–16

Original Article

Comparison of spinal vasculature in mouse and rat: investigations using MR angiography

Published online 3 March, 2006 © http://www.neuroanatomy.org

Mehmet BILGEN [1, 2] ✦
Baraa AL-HAFEZ [1]

Hoglund Brain Imaging Center [1]; Department of Molecular and Integrative Physiology [2], The University of Kansas Medical Center, Kansas City, USA.

✦ Mehmet Bilgen, Ph.D.,
Hoglund Brain Imaging Center, Mail Stop 1052
3901 Rainbow Blvd
Kansas City, KS 66160, USA.
☎ +1 (913) 588-90 79
+1 (913) 588-90 71
✉ mbilgen@kumc.edu

Received 15 January 2006; accepted 27 February 2006

ABSTRACT

The first goal of this work is to demonstrate the feasibility of performing three-dimensional, time-of-flight magnetic resonance angiography (MRA) on the spine and spinal cord (SC) of mouse. The MRA studies were performed at 9.4 T magnetic field strength using a custom designed inductively coupled surface coil. The results of the present study demonstrate the possibility of remotely imaging the arteries supplying blood to the mouse spine and spinal cord at high spatial resolution and high signal-to-noise ratio. Data also show that the arteries in the parenchyma of the SC are highly organized with projections at multiple levels along the cord, as originating from the anterior spinal artery. The second goal is to compare the arterial organization in mouse and rat at the spinal level and to explain cause-and-effect relationship to examine the differences observed in the neuropathologies following spinal cord injury in these species. ***Neuroanatomy; 2006; 5: 12–16.***

Key words [magnetic resonance imaging] [angiography] [inductively coupled surface coil] [spine] [spinal cord] [spinal vasculature]

Introduction

The spinal vascular system is the conduit through which nutrition, cells and drugs access the parenchyma of the spinal cord (SC). This system is severely damaged as a principal consequence of the spinal cord injury (SCI). The initial vascular damage plays a critical role in establishing the course of the well-established postinjury cascade including compromised blood spinal cord permeability, hypoxia, activation of various factors and, subsequently, secondary injuries [1–6].

Rodent models play an important role in experimental studies of SCI [7, 8]. Rat model of SCI is more representative of what occurs in most closed human injuries. In this model, evolution of the neuropathology over time begins with an early phase of spreading hemorrhagic necrosis and edema, progressing to an intermediate phase of partial repair and tissue reorganization, and reaching a chronic phase characterized by the establishment of central cystic cavities with atrophic parenchyma and glial scarring. Recent trends indicate that mouse models of SCI are becoming more common [9–17]. The main reason behind this shift of focus is that genetically engineered mice offer opportunities to study the role of particular genes in the pathophysiology of SCI and thereby allow the development of more specific treatment strategies [18]. However, it is also recognized that the neuropathology of injured SC in mouse exhibits distinctly different spatio-temporal course than what is observed in rat. Specifically, mice exhibit a unique wound-healing response with typical characteristics of lesion site filling in with fibrous connective tissue matrix [9, 10, 19–23]. Magnetic resonance images can sensitively detect the differences between these pathological patterns in moderate injuries, induced with the device described in [17], in rat and mouse SCs (see Fig. 1).

It is conceivable that the observed differences in the injury responses in mice and rats may be due to species-specific differences in the vascular organization of the spine. This establishes a strong motivation to study the arterial formation supplying blood from the descending aorta to the pial arteries as well as the distribution of blood in the parenchyma of the SC. We hypothesize that if the arterial vascularization (intra- and extra-parenchymal) were different in normal animals, the pathophysiology following an injury would naturally be different. These differences may subsequently lead to the specific neuropathological responses observed in injured mice and rats. Therefore, our aim in this study is to test this hypothesis by using magnetic resonance angiography (MRA) as an in vivo imaging tool to visualize the organization of the arterial network in normal mouse spine and parenchyma, and compare it with that of normal rat.

Material and Methods

All MRI scans were performed on a *9.4 T* INOVA Varian system (Varian Inc., Palo Alto, CA) with 31 cm horizontal bore magnet. The data were acquired from

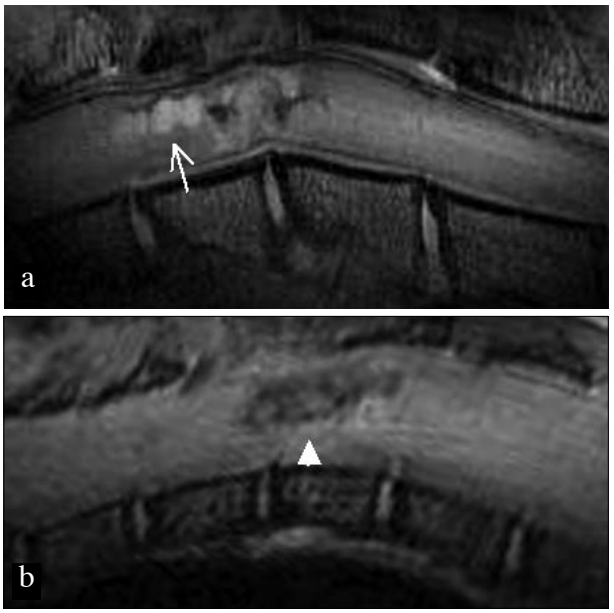

Figure 1. *In vivo* sagittal MRIs showing the pathology of injured spinal cords in ***(a)*** rat and ***(b)*** mouse on its chronic phase. Arrow points to the formation of a cystic cavity appearing hyperintense on the rat spinal cord image. Arrowhead points to the formation of a scar appearing hypointense on the mouse spinal cord image.

male C57Bl/6 mice and Sprague Dawley rats using an inductively coupled surface coil that was placed adjacent to the spine at the thoracic level. The placement of the coil to image the spine, optimization of its tuning at the resonant frequency, and matching its impedance when operated in combination with the pickup coil were carried out according to the published procedures [24]. The animals were scanned while under isoflurane anesthesia (a mixture of 1.5% isoflurane, 30% oxygen, and air) administrated via a facemask under an experimental protocol approved by the *University of Kansas Medical Center Institutional Animal Care and Use Committee* (IACUC). The physiological condition of the animal was monitored using ECG, respiratory and temperature probes that were connected to an MR-compatible small animal monitoring and gating system (Model 1025, SA Instruments, Inc., Stony Brook, NY). The temperature of the mouse was kept at 37 °C by circulating warm air with 40% humidity using a 5 cm diameter plastic tubing fitted at the back door of the magnet bore.

The Plexiglass sled supporting the animal and the coil was inserted into the scanner bore, and its proper placement at the magnet isocenter was confirmed with scout images. High-resolution anatomical images were then acquired in multi-slice and interleaved fashion in axial, sagittal, and coronal planes using a standard spin echo (SE) sequence with T_R/T_E = 2000/13 ms, acquisition matrix = 128x128, image matrix = 256x256, slice thickness = 1 mm and NEX = 2. Field-of-view (FOV) was 9x9 mm^2 for the axial and 9x25 mm^2 for the coronal and sagittal images. Next, angiograms were acquired using the 3D-TOF sequence [25]. The values for the MRA parameters were T_R/T_E = 45/4 ms and flip angle (FA) = 45°, and applied over a volume of 18x18x9 mm^3, where the former

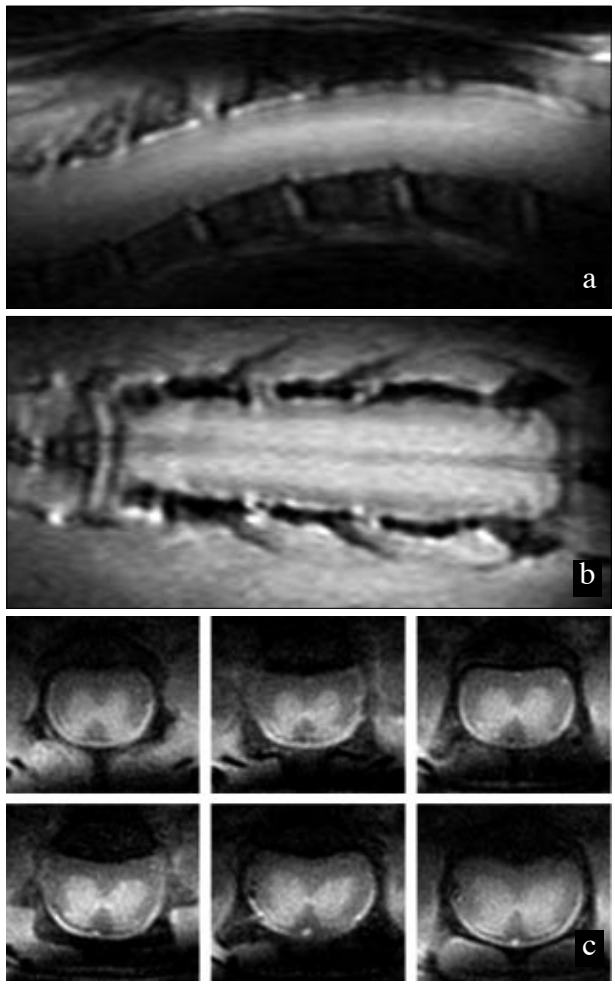

Figure 2. *In vivo* spin-echo MRIs showing the anatomy of the mouse spinal cord in ***a)*** sagittal, ***b)*** coronal and ***c)*** axial planes.

represents the readout direction. The raw data were digitized at a sampling rate of 128x128x64. A selective excitation centered on the second phase encode direction was applied over a slab thickness of 7 mm. With these settings, the total acquisition time was about 12 min 20 s, and the spatial pixel resolution was about 140 um in all directions. Rat MRAs were acquired with 128x128x128 samples over a volume of 25x20x20 mm^3 and 16 mm of slab thickness.

The acquired MRA data were processed and interpolated to a matrix size of 256x256x128 pixels for mouse and 256x256x256 pixels for rat and maximum intensity projections were generated as angiograms in the coronal, sagittal, and axial views.

Results

Typical anatomical images of the mouse SC acquired with the setup described above are shown in Figure 2. The high-resolution images delineate the anatomical details of the cord at the thoracic level in different views and also provide a reference for the description of the data in the following. A set of representative spinal angiograms in Figure 3 shows the arterial architecture in mouse spine. Clearly, the vascular organization of the mouse vertebral column and SC consists of a complex network of arteries

delivering blood to the SC from multiple directions and levels. Anatomically, the *posterior intercostal artery* (PIC) originates from *aorta* and branches into smaller projections, such as the *dorsal branch* (DB), *anterior radicular artery* (ARA) and *anterior spinal artery* (ASA). As in humans, a single artery, similar to the artery of *Adamkiewicz*, supplies blood to the ASA at the thoracolumbar level. The ASA longitudinally runs along the cord, as is the *posterior spinal artery* (PSA) on the dorsal site.

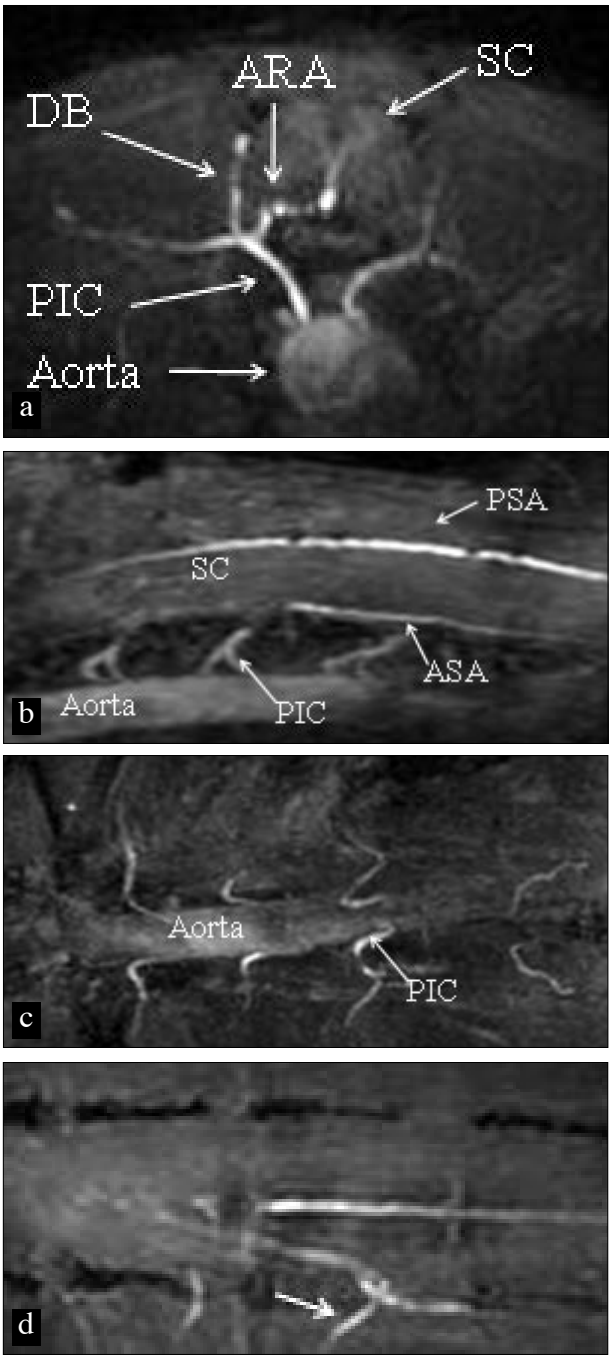

Figure 3. Angiograms showing the anatomy of arteries supplying blood to the mouse spinal cord in ***(a)*** axial, ***(b)*** sagittal and ***(c)*** coronal planes. Top image shows the posterior section with respect to the mouse body. ***PIC*** indicates the *posterior intercostal arteries*, originating from the aorta at different thoracic levels, ***DB*** denotes its *dorsal branch*, ***ARA*** is the *anterior radicular artery*, ***ASA*** is the *anterior spinal artery* and ***PSA*** *posterior spinal artery*. The arrow in ***(d)*** points to ***ARA*** (the equivalent of the *great ventral radicular artery* of Adamkiewicz in humans) entering into the spinal canal through the intervertebral foramina, continue along the nerve root to feed the pial ASA as a single vessel at the thoracic level.

For the purpose of emphasizing the blood flow in the parenchyma of the SC, we shifted the selective excitation band closer to the posterior surface and produced the angiograms in Figures 4–6. In the sagittal planes (Fig. 4), the parenchymal arteries are structurally seen as branching from the ASA and projecting radially inwards in a comb-like fashion. The coronal images (Fig. 5) confirm this arrangement and outline these vessels as a group of periodically separated bright hot spots in the midline of the SC. Along the same lines, the axial views (Fig. 6) delineate some of these perforating vessels penetrating deeply into the parenchyma of the cord by the way of the anterior median fissure to a final distribution in the gray matter.

Compared to mouse, vasculature in rat spine exhibits close similarity in terms of its anatomical organization. In rat, SC receives blood from major external arteries, ARA and PIC, originating from the aorta, and the arteries ASA and PSA, as well as smaller arteries on the pial surface of the SC (Fig. 7). Parenchymal SC tissue receives blood from small arterial projections originating from the ASA and penetrating radially, as shown in Figure 8.

Discussion

Taken together, our data collectively demonstrate the feasibility of performing high quality *in vivo* MRA on the

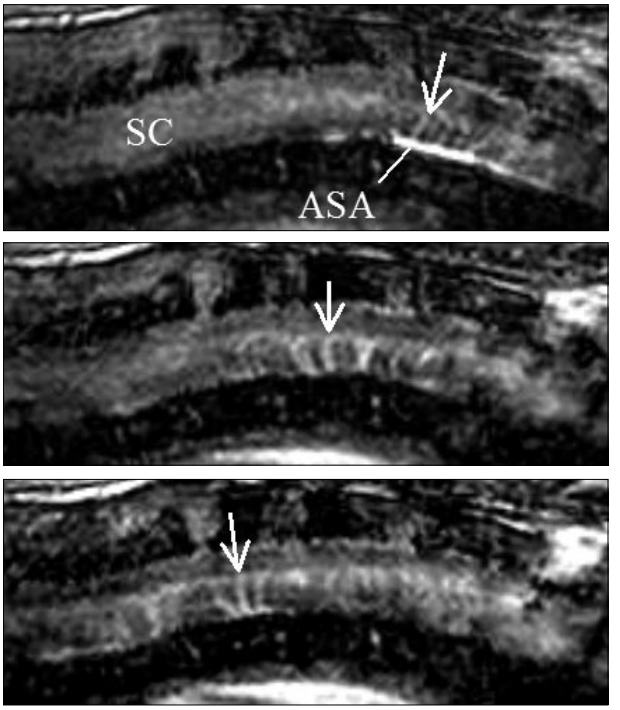

Figure 4. Sagittal angiograms showing the parenchymal arteries of mouse spinal cord ***(arrows)***. These arteries branch off the anterior spinal artery and project radially in the parenchyma of the cord. The arteries appear as a comb-like shape in the midline of the cord.

spine and SC of mouse. Dealing with small size mouse was challenging in some regards, but also offered some advantages. To acquire high quality anatomical data, we have implemented the necessary components in our imaging setup and employed several strategies that have proven to be beneficial. The characteristics of high SNR and improved sensitivity in the custom designed rf coil allowed acquiring images with small FOV (9x9 mm^2), but also produced an inherently non-uniform excitation profile and reception sensitivity. As in the case of MRA studies on rat SC [25], incomplete suppression of the background tissue was evident on the mouse angiograms

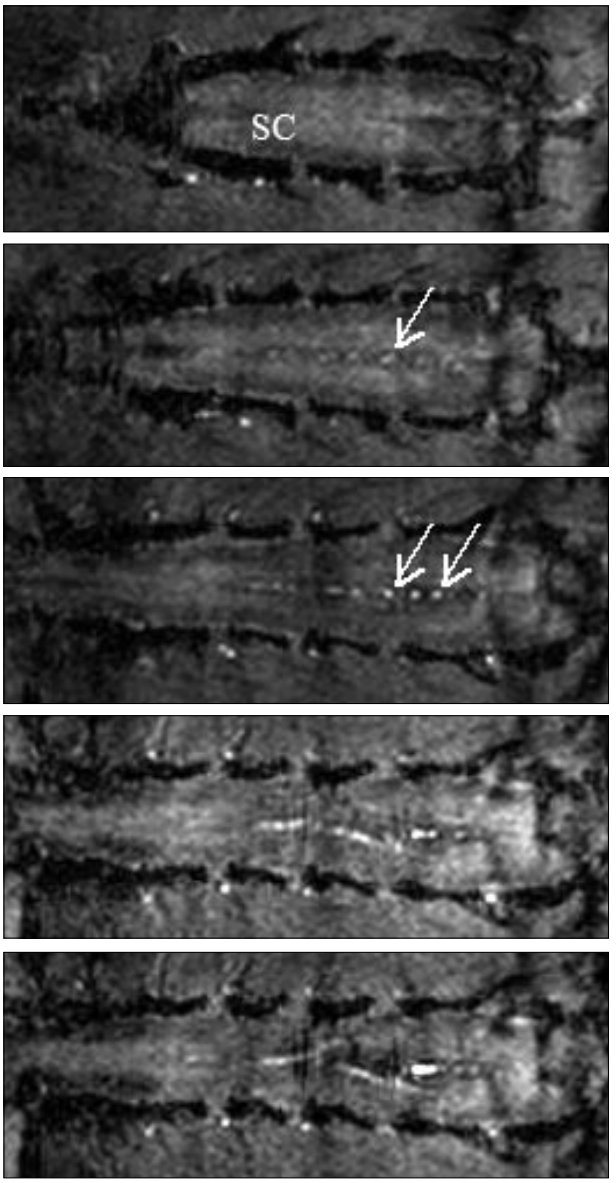

Figure 5. Coronal view of the parenchymal arteries of mouse spinal cord ***(arrows)***. The images from top to bottom represent coronal slices from posterior to anterior.

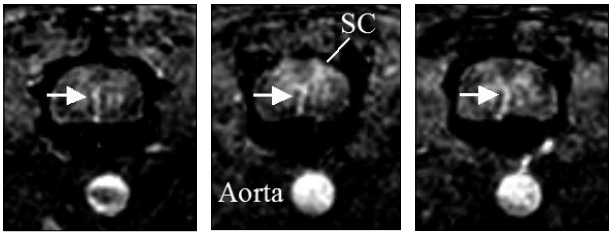

Figure 6. Axial views of three arteries ***(arrows)*** in the parenchyma of mouse spinal cord.

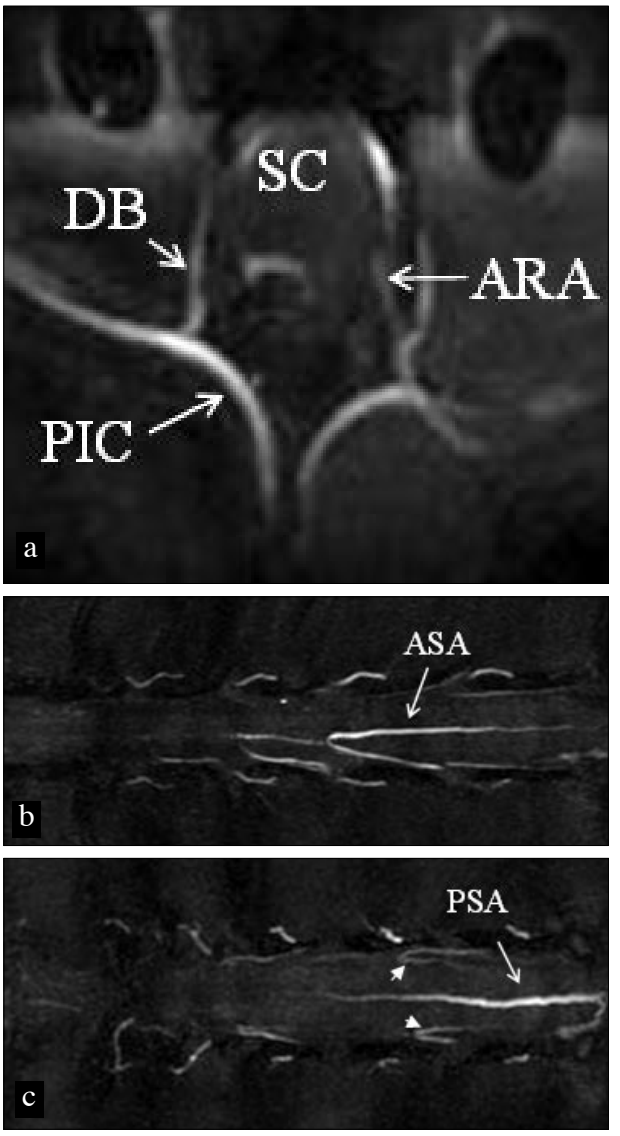

Figure 7. Angiograms showing the anatomy of arteries on ***(a)*** axial view and ***(b)*** anterior and ***(c)*** posterior half of the rat spinal cord in coronal views. ***Arrowheads*** in (c) point to the projections of the smaller arteries on the pial surface.

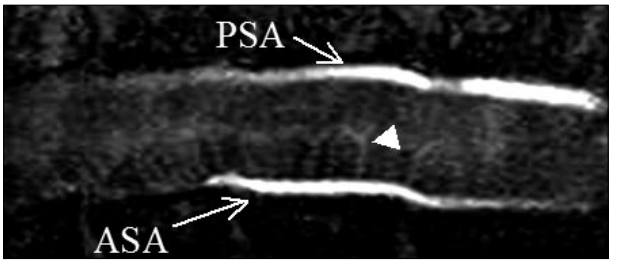

Figure 8. Sagittal angiogram showing the parenchymal arteries of rat spinal cord ***(arrow head)***.

but with less severity. The angiograms has shown regional sensitivity to the inflow of the unsaturated spins in the freshly supplied blood, but was compensated by optimizing the imaging parameters accordingly.

We investigated if the differences between the anatomical organization of the arterial network in mice and rat spine may (directly or indirectly) lead to unique neuropathologies seen in these species following SCI. Inner variability exists in local microcirculation within the parenchyma of the SC in each species. Our current capabilities are limited in providing such information. However, concerning the part that covers the major arteries and their organization from aorta to the branches of ASA, our data indicate that mice and rats have similar arterial networks. This observation is in agreement with the previous report based on the histological examination [26], and suggests minimal participation of this network in defining the neuropathological responses seen in these species following SCI. Previously, it has also been reported that the physical size of the SC is not to be the factor determining the course of the neuropathology following the injury in mouse [23].

Conclusion

Experimental studies of SCI increasingly employ genetically engineered mice as a model animal, while more frequent use of conventional MRI of mouse SC is also becoming more common [27, 28]. We anticipate that the addition of high resolution MRA scans will enhance the capabilities of the existing imaging protocols in these experimental studies. In research aimed at understanding the natural, perturbed or intervened evolution of the postinjury vascular processes on the same animal [6, 29–33], MRA, in particular, can potentially play an important role by providing a robust longitudinal modality for imaging these processes in mouse models of SCI.

Acknowledgments

The author thanks *Dr Carmen Cirstea* and *Melanie Doerflinger* for providing editorial help.

References

[1] **Tator CH.** Review of experimental spinal cord injury with emphasis on the local and systemic circulatory effects. **Neurochirurgie. 1991; 37: 291–302.**

[2] **Tator CH, Koyanagi I.** Vascular mechanisms in the pathophysiology of human spinal cord injury. J. Neurosurg. **1997; 86: 483–492.**

[3] **Imperato-Kalmar EL, McKinney RA, Schnell L, Rubin BP, Schwab ME.** Local changes in vascular architecture following partial spinal cord lesion in the rat. **Exp. Neurol. 1997; 145: 322–328.**

[4] **Mautes AE, Weinzierl MR, Donovan F, Noble LJ.** Vascular events after spinal cord injury: contribution to secondary pathogenesis. **Phys. Ther. 2000; 80: 673–687.**

[5] **Westergren H, Farooque M, Olsson Y, Holtz A.** Spinal cord blood flow changes following systemic hypothermia and spinal cord compression injury: an experimental study in the rat using Laser-Doppler flowmetry. **Spinal Cord. 2001; 39: 74–84.**

[6] **Whetstone WD, Hsu JY, Eisenberg M, Werb Z, Noble-Haeusslein LJ.** Blood-spinal cord barrier after spinal cord injury: relation to revascularization and wound healing. **J. Neurosci. Res. 2003; 74: 227–239.**

[7] **Kwon BK, Oxland TR, Tetzlaff W.** Animal models used in spinal cord regeneration research. **Spine. 2002; 27: 1504–1510.**

[8] **Rosenzweig ES, McDonald JW.** Rodent models for treatment of spinal cord injury: research trends and progress toward useful repair. **Curr. Opin. Neurol. 2004; 17: 121–131.**

[9] **Kuhn PL, Wrathall JR.** A mouse model of graded contusive spinal cord injury. **J. Neurotrauma. 1998; 15: 125–140.**

[10] **Ma M, Basso DM, Walters P, Stokes BT, Jakeman LB.** Behavioral and histological outcomes following graded spinal cord contusion injury in the C57Bl/6 mouse. **Exp. Neurol. 2001; 169: 239–254.**

[11] **Seitz A, Aglow E, Heber-Katz E.** Recovery from spinal cord injury: a new transection model in the C57Bl/6 mouse. **J. Neurosci. Res. 2002; 67: 337–345.**

[12] **Seki T, Hida K, Tada M, Koyanagi I, Iwasaki Y.** Graded contusion model of the mouse spinal cord using a pneumatic impact device. **Neurosurgery. 2002; 50: 1075–1081; discussion 1081–1072.**

[13] **Joshi M, Fehlings MG.** Development and characterization of a novel, graded model of clip compressive spinal cord injury in the mouse: Part 1. Clip design, behavioral outcomes, and histopathology. **J. Neurotrauma. 2002; 19: 175–190.**

[14] **Joshi M, Fehlings MG.** Development and characterization of a novel, graded model of clip compressive spinal cord injury in the mouse: Part 2. Quantitative neuroanatomical assessment and analysis of the relationships between axonal tracts, residual tissue, and locomotor recovery. **J. Neurotrauma. 2002; 19: 191–203.**

[15] **Anderson KD, Abdul M, Steward O.** Quantitative assessment of deficits and recovery of forelimb motor function after cervical spinal cord injury in mice. **Exp. Neurol. 2004; 190: 184–191.**

[16] **Sheng H, Wang H, Homi HM, Spasojevic I, Batinic-Haberle I, Pearlstein RD, Warner DS.** A no-laminectomy spinal cord compression injury model in mice. **J. Neurotrauma. 2004; 21: 595–603.**

[17] **Bilgen M.** A new device for experimental modeling of central nervous system injuries. **Neurorehabil. Neural Repair. 2005; 19: 219–226.**

[18] **Guertin PA.** Paraplegic mice are leading to new advances in spinal cord injury research. **Spinal Cord. 2005; 43: 459–461.**

[19] **Zhang Z, Fujiki M, Guth L, Steward O.** Genetic influences on cellular reactions to spinal cord injury: a wound-healing response present in normal mice is impaired in mice carrying a mutation (WldS) that causes delayed Wallerian degeneration. **J. Comp. Neurol. 1998; 371: 485–495.**

[20] **Steward O, Schauwecker PE, Guth L, Zhang Z, Fujiki M, Inman D, Wrathall J, Kempermann G, Gage FH, Saatman KE, Raghupathi R, McIntosh T.** Genetic approaches to neurotrauma research: opportunities and potential pitfalls of murine models. **Exp. Neurol. 1999; 157: 19–42.**

[21] **Sroga JM, Jones TB, Kigerl KA, McGaughy VM, Popovich PG.** Rats and mice exhibit distinct inflammatory reactions after spinal cord injury. **J. Comp. Neurol. 2003; 462: 223–240.**

[22] **Inman DM, Steward O.** Ascending sensory, but not other long-tract axons, regenerate into the connective tissue matrix that forms at the site of a spinal cord injury in mice. **J. Comp. Neurol. 2003; 462: 431–449.**

[23] **Inman DM, Steward O.** Physical size does not determine the unique histopathological response seen in the injured mouse spinal cord. **J. Neurotrauma. 2003; 20: 33–42.**

[24] **Bilgen M.** Simple, low-cost multipurpose RF coil for MR microscopy at 9.4 T. **Magn. Reson. Med. 2004; 52: 937–940.**

[25] **Bilgen M, Al-Hafez B, He YY, Brooks WM.** Magnetic resonance angiography of rat spinal cord at 9.4 T: a feasibility study. **Magn. Reson. Med. 2005; 53: 1459–1461.**

[26] **Lang-Lazdunski L, Matsushita K, Hirt L, Waeber C, Vonsattel JP, Moskowitz MA, Dietrich WD.** Spinal cord ischemia. Development of a model in the mouse. **Stroke. 2000; 31: 208–213.**

[27] **Bonny JM, Gaviria M, Donnat JP, Jean B, Privat A, Renou JP.** Nuclear magnetic resonance microimaging of mouse spinal cord in vivo. **Neurobiol. Dis. 2004; 15: 474–482.**

[28] **Bilgen M, Al-Hafez B, Berman NEJ, Festoff BW.** Magnetic resonance imaging of mouse spinal cord. **Magn. Reson. Med. 2005; 54: 1226–1231.**

[29] **Beggs JL, Waggener JD.** Microvascular regeneration following spinal cord injury: the growth sequence and permeability properties of new vessels. **Adv. Neurol. 1979; 22: 191–206.**

[30] **Casella GT, Marcillo A, Bunge MB, Wood PM.** New vascular tissue rapidly replaces neural parenchyma and vessels destroyed by a contusion injury to the rat spinal cord. **Exp. Neurol. 2002; 173: 63–76.**

[31] **Facchiano F, Fernandez E, Mancarella S, Maira G, Miscusi M, D'Arcangelo D, Cimino-Reale G, Falchetti ML, Capogrossi MC, Pallini R.** Promotion of regeneration of corticospinal tract axons in rats with recombinant vascular endothelial growth factor alone and combined with adenovirus coding for this factor. **J. Neurosurg. 2002; 97: 161–168.**

[32] **Loy DN, Crawford CH, Darnall JB, Burke DA, Onifer SM, Whittemore SR.** Temporal progression of angiogenesis and basal lamina deposition after contusive spinal cord injury in the adult rat. **J. Comp. Neurol. 2002; 445: 308–324.**

[33] **Benton RL, Whittemore SR.** VEGF165 therapy exacerbates secondary damage following spinal cord injury. **Neurochem. Res. 2003; 28: 1693–1703.**